Published online: September 30, 2020

Original Research

Clathrin-independent but dynamin-dependent mechanisms mediate Ca^{2+}-triggered endocytosis of the glutamate GluK2 receptor upon excitotoxicity

Jing-Jing Du[1], Lu Yan[1], Wei Zhang[1], Hao Xu[1,2], and Qiu-Ju Zhu[1,2,*]

[1]*Jiangsu Key Laboratory of Brain Disease Bioinformation, Xuzhou Medical University, Jiangsu, 221004, P. R. China*

[2]*Research Center for Biochemistry and Molecular Biology, Xuzhou Medical University, Jiangsu, 221004, P. R. China*

*Correspondence: zhuqiuju@xzhmu.edu.cn (Qiu-Ju Zhu)

DOI:10.31083/j.jin.2020.03.99

We first explore the features of GluK2 endocytosis during kainate excitotoxicity and then explore the role of Ca^{2+} in the regulation of GluK2 endocytosis. The roles of Ca^{2+} were examined by treating cells with Ca^{2+} inhibitors or chelators. Surface biotinylation was used to examine the surface localization of GluK2. Immunoprecipitation followed by immunoblotting was used to identify the interaction of GluK2 with the endocytosis regulator protein-interacting with C kinase 1 and dynamin. Dynamin phosphorylation was examined by immunoblotting with the corresponding antibodies. Our results show that GluK2 internalization is blocked by inhibitors of clathrin-independent endocytosis and relies on intracellular Ca^{2+}/calcineurin signaling. Protein-interacting with C kinase 1-GluK2 interaction is regulated by Ca^{2+}/calcineurin signaling. Dynamin participates in the regulation of GluK2 surface localization. Also, calcineurin activation is related to dynamin function during kainate excitotoxicity. In conclusion, GluK2 receptor endocytosis is probably a clathrin-independent and dynamin-dependent process regulated by the peak Ca^{2+} transient. This work indicates the roles of the Ca^{2+} network in the regulation of GluK2 endocytosis during kainate excitotoxicity.

Keywords

GluK2 endocytosis; Calcium; calcineurin; excitotoxicity

1. Introduction

Glutamate receptors include the α-amino-3-hydroxy-5-methyl-4-isoxazolepropionic acid receptor (AMPAR), the N-methyl-d-aspartate receptor (NMDAR), and the kainate receptor (KAR). KARs are localized both presynaptically and postsynaptically, affecting transmitter release and are responsible for slow excitatory postsynaptic currents (EPSCs) (Huettner, 2003; Kerchner et al., 2002; Lerma, 2003; Vignes and Collingridge, 1997). There are five types of subunits in KARs: GluK1-5. The GluK1-3 subunits constitute the functional KAR, whereas the GluK4 and GluK5 subunits need to combine with GluK1-3. The GluK2 subunit has been proven to control synaptic integration and spike transmission at hippocampal mossy fiber synapses (Sachidhanandam et al., 2009). In GluK2-deficient mice, the presynaptic action of KAR is lost (Contractor et al., 2001), and the KAR component of EPSC is absent (Mulle et al., 1998). The GluK2 antisense oligodeoxynucleotides exert neuroprotective effects on neuronal death in the rat hippocampal CA1 region after transient brain ischemia/reperfusion (Pei et al., 2006). All of these findings suggest a critical role of GluK2 in physiological and pathological neuronal functions.

As arborized and polarized cells, neurons exhibit endocytic features related to their specific physiological and pathological functions. Studies have demonstrated that the process of glutamate receptor endocytosis is crucial for neuronal function and excitotoxicity (Malinow and Malenka, 2002; Man et al., 2000; Wang et al., 2004; Zhu et al., 2012). The surface localization of GluK2 determines the responsiveness of neurons and profoundly influences signal transduction of neurons (Martin et al., 2007; Zhu et al., 2012). Evidence shows that GluK2 receptor endocytosis is regulated by posttranslational modification (Konopacki et al., 2011; Nasu-Nishimura et al., 2010; Zhu et al., 2014, 2012). However, the molecular events in the GluK2 endocytic process have not been defined.

Calcium (Ca^{2+}) imbalance is a significant trigger that leads to neuronal cell death during brain damage, and its inhibition directly correlates with ischemic neuroprotection (Berliocchi et al., 2006; Choi, 1995; Tymianski et al., 1993). Different synaptic preparation studies have shown that Ca^{2+} can accelerate or inhibit endocytosis at nerve terminals (Balaji et al., 2008; Wu et al., 2009, 2014; Yao and Sakaba, 2012); nevertheless, the precise steps by which Ca^{2+} acts in this process have not been identified. Calcineurin (CaN), a calcium/calmodulin-activated phosphatase that dephosphorylates endocytosis-related proteins, has long been suspected of mediating this Ca^{2+}-regulated process (Cousin and Robinson, 2001). However, whether CaN mediates endocytic processes is highly controversial (Wu et al., 2014). KAR desensitization plays a vital role in kainate-induced increases in intracellular free Ca^{2+}, and GluK2 subunits are Ca^{2+}-permeable (Ouardouz et al., 2009; Silva et al., 2001). In cells expressing the tyrosine phosphorylation-deficient GluK2 mutant Y590F, both GluK2 endocytosis and peak

Journal of Integrative Neuroscience

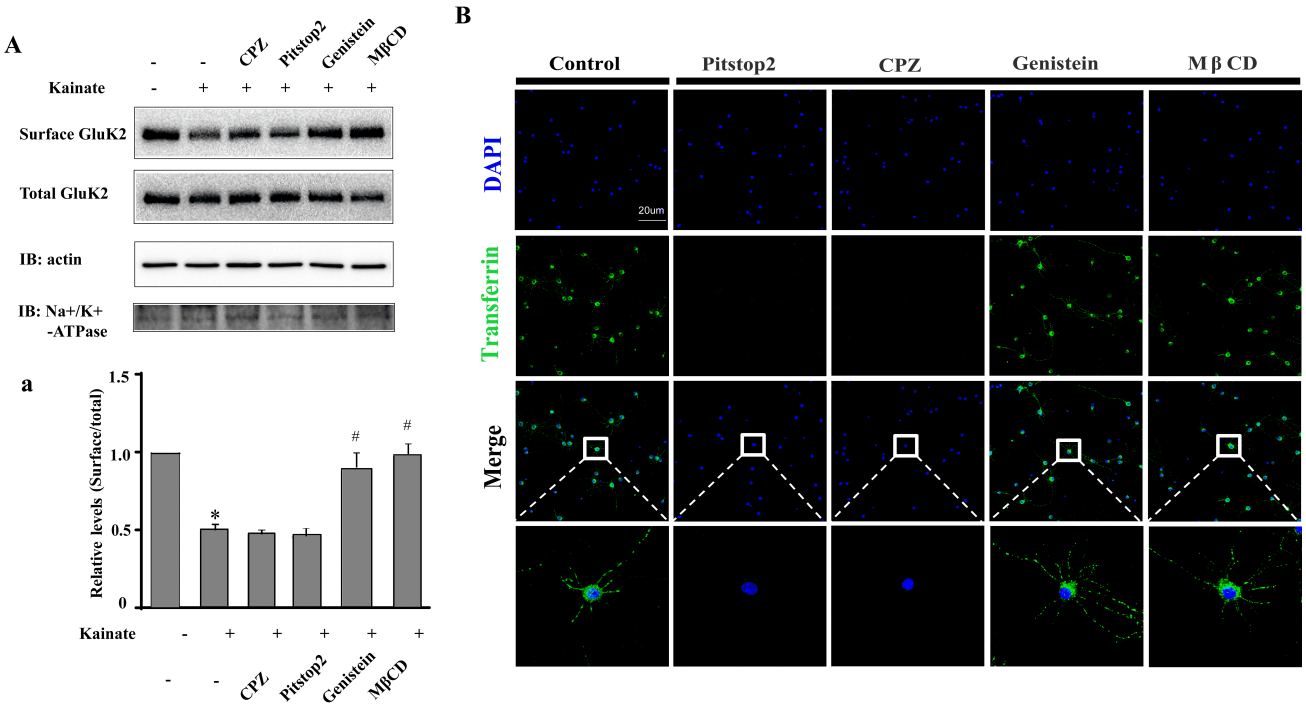

Fig. 1. GluK2 endocytosis is prevented by genistein or MβCD but not by CPZ or pitstop2. Cultured cortical neurons were pretreated with CPZ (10 μmol/L), pitstop2 (25 μmol/L), genistein (200 μmol/L), or MβCD (3 mmol/L) for 30 min before kainate stimulation (300 μmol/L, 10 min) or transferrin binding (20 μg/ml, 10 min). (A) The surface and total GluK2 were immunoblotted with an anti-GluK2/3 antibody. The surface/total ratios of GluK2 are normalized to that of the control (without kainate stimulation) and expressed as the mean $\pm$ SD (n = 3). $^{*}P < 0.05$ vs. no kainate. $^{\#}P < 0.05$ vs. no inhibitor in kainate stimulation. Neuron cultures for replicates were made from different animals. (B) The endocytosis assay of Alexa 488-conjugated transferrin in cortical neurons confirms the specificity of the inhibitors. Neuron cultures for replicates were made from different animals.

transients of intracellular Ca^{2+} are inhibited (Zhu et al., 2014). Therefore, a better understanding of the dysregulation of Ca^{2+} and its roles in GluK2 endocytosis can provide evidence about the role of Ca^{2+} during GluK2-mediated excitotoxicity.

2. Materials and methods

2.1 Antibodies and reagents

Rabbit polyclonal anti-protein-interacting with C kinase 1 (PICK1) (ab3420), anti-dynamin1 (ab3456), anti-dynamin1 phospho-Ser-774 (ab55324) and pitstop2 were obtained from Abcam Biotechnology (Cambridge, UK). Sheep polyclonal anti-dynamin phospho-Ser-778 (NB300-210) was obtained from Novus Biotechnology (Littleton, CO, USA). Rabbit monoclonal anti-GluK2/3 (clone NL9, #04-921) antibodies were purchased from Millipore Biotechnology (Temecula, CA, USA). Rabbit polyclonal anti-actin (sc-10731) was obtained from Santa Cruz Biotechnology (Dallas, TX, USA). Rabbit polyclonal Na^{+}/K^{+}-ATPase (#3010) was purchased from Cell Signaling Biotechnology. Kainate receptor agonist was purchased from Enzo life sciences (Farmingdale, NY, USA). Chlorpromazine hydrochloride (CPZ), genistein, methyl-β-cyclodextrin (MβCD), dynasore (D7693), dantrolene (Dan), ryanodine (Rya), FK506, and Fura-2/AM were from Sigma-Aldrich Biotechnology (St. Louis, MO, USA). Cyclosporine A (CsA) was obtained from EMD Millipore (Billerica, MA, USA). Alexa Fluor 488-conjugated transferrin (T13342) and EZ link sulfo-NHS-SS-Biotin (21331) was from Thermo Scientific (Rockford, IL, USA).

2.2 Plasmid transfection and drug administration

HEK293T cells were obtained from the American Type Culture Collection (Manassas, VA, USA) and were cultured in DMEM supplemented with 10% FBS. The recombinant plasmids encoding GluK2 (the wild-type protein and the tyrosine phosphorylation-deficient mutant Y590F) were introduced into the cells with polyethyleneimine (PEI; Invitrogen). After transfection (24 h), drugs were administered to the transfected cells.

2.3 Calcium imaging

Intracellular Ca^{2+} ($[Ca^{2+}]_i$) was measured using the Ca^{2+}-sensitive fluorescent dye Fura-2/AM (Sigma), which is a UV-excited Ca^{2+} indicator that allows for ratiometric measurements. Fura-2/AM was dissolved in DMSO as a stock solution and directly added to the cell culture medium at a final concentration of 2 μM. After GluK2 transfection (24 h), HEK293T cells were loaded with Fura-2/AM for 30 min at room temperature and then washed three times to remove the extracellular dye. The Fura-2 fluorescence was alternately excited at 340 and 380 nm using the Lambda DG-4 Ultra-High-Speed Wavelength Switcher, and the excitation light was focused on the cells via a 20$\times$ objective. The emitted fluorescence was collected at 510 nm by a high-speed EMCCD camera. The ratio of the fluorescence at 340 nm to 380 nm was directly recorded with Meta Fluor software, indicating $[Ca^{2+}]_i$) fluctuations. The intracellular free calcium concentration ($[Ca^{2+}]_i$)) was calculated as follows: $[Ca^{2+}]_i$) = Kd[(R-Rmin)/(Rmax-R)]β

(Grynkiewicz et al., 1985; Xu et al., 2012), where R is the ratio of fluorescence emitted at 510 nm after excitation at 340 and 380 nm; Rmin is the ratio of fluorescence at zero calcium, and Rmax is the ratio at saturating calcium. Kd is the effective dissociation constant of Fura-2 for calcium and is equal to 224 nmol/L. β is the ratio of fluorescence of Fura-2 at 380 nm in the presence of EGTA to that in the presence of ionomycin and is equal to 1.53. Rmax and Rmin were determined by the ionomycin method.

2.4 Cortical neuron culture

Primary cortical neurons from 18-d-old embryonic Sprague Dawley rats were seeded in poly-D-lysine-coated culture dishes at 0.8×105 cells/cm^2 as previously described (Xu et al., 2009). The culture medium (Neuro-basal medium supplemented with 2% B27 and 0.5 mM glutamine) was replaced every 3 days. After 14 days of *in vitro* culture, the neurons were harvested and lysed in ice-cold homogenization buffer [in mmol/L: MOPS (pH 7.4) 50, sucrose 320, KCl 100, $MgCl_2$ 0.5, and protease and phosphatase inhibitors (β-glycerophosphate 20; sodium pyrophosphate 20; NaF 50; 1 mmol/L each of EDTA, EGTA, phenylmethylsulfonyl fluoride, benzamidine, sodium orthovanadate, and p-nitrophenyl phosphate; and 5 μg/mL each of aprotinin, leupeptin, and pepstatin A)] to be used for the experiments.

2.5 Transferrin uptake assay

The transferrin-endocytosis assay was performed as previously described (Fu et al., 2011; Lu et al., 2016; Mackenzie et al., 2017). After 7 days of *in vitro* culture, the primary cortical neurons were starved in a neuro-basal medium for 2 h. For the uptake assays, the starved cells were transferred to a binding media (neuro-basal medium with 0.2% bovine serum albumin, 20 mM HEPES-NaOH [pH 7.5]) containing 20 μg/ml human transferrin-Alexa Fluor 488 (Thermo, Waltham, MA USA) and placed in an incubator with 95% O_2, 5% CO_2 for 30 min. The neurons were washed with ice-cold PBS three times and then fixed with 4% paraformaldehyde in $1\times$ PBS. Confocal images were acquired using a Zeiss LSM710 laser-scanning confocal microscope (Zeiss, Germany).

2.6 Surface biotinylation

Live transfected HEK293T cells, and primary cortical neurons were surface-biotinylated on ice using EZ link sulfo-NHS-SS-Biotin (Pierce) (Rockford, IL) after kainate stimulation with or without inhibitor treatments. The harvested cells were lysed in TNE buffer [50 mmol/L Tris·HCl (pH 8.0), 50 mmol/L NaF, 1% Nonidet P-40, 20 mmol/L EDTA, and 0.1% SDS]. The cell lysates (200 μg) were incubated with 30 μL of immobilized NeutrAvidin (Pierce), which binds specifically to sulfo-NHS-SS-Biotin, at 4 °C for 2 h to precipitate the biotinylated proteins. The immobilized NeutrAvidin were washed three times to remove the nonspecifically bound proteins and collect the surface proteins. The surface proteins bound to the immobilized NeutrAvidin and the total cell lysates were boiled at 100 °C for 5 min and subjected to immunoblot analysis with anti-GluK2 antibodies.

2.7 Immunoprecipitation

The sample proteins were incubated with the appropriate antibodies diluted in immunoprecipitation buffer (the ratio was 1 μg antibody per 400 μg protein in 400 μl buffer) containing 50 mmol/L HEPES (pH 7.4), 150 mmol/L NaCl, 10% glycerol (vol/vol), 1 mmol/L $ZnCl_2$, 1.5 mmol/L $MgCl_2$, 1% Triton X-100, 0.5% Nonidet P-40, and the phosphatase and protease inhibitors mentioned above overnight at 4 °C (Zhu et al., 2012). The mixture was incubated at 4 °C for an additional 2 h after the addition of protein A/G. The samples were washed with immunoprecipitation buffer three times and eluted by boiling for 5 min at 100 °C in $4\times$ Laemmli sample buffer.

2.8 Immunoblot

After boiling at 100 °C for 5 min, the immuno-precipitates or equal amounts of the sample proteins were separated by SDS-PAGE and then electrotransferred onto a nitrocellulose membrane (pore size: 0.22 μm). After blocking in 3% bovine serum albumin (BSA), the membrane was incubated with the indicated primary antibodies overnight at 4 °C. Detection was performed with the appropriate HRP-conjugated IgG and developed with the SuperSignal™ West Pico Chemiluminescent Substrate assay kit (#34087) (Thermo Fisher Scientific). The bands on the membranes were scanned and analyzed with Quantity One 1-D Analysis Software (Bio-Rad).

2.9 Statistical analysis

For each type of experiment, the data were obtained from at least three independent measurements. Except for peak Ca^{2+} transient in calcium imaging, data were normalized to the corresponding control in each experiment before statistical analysis. The student's *t*-test evaluated differences between the means of two groups. Multiple groups were compared by one-way ANOVA, followed by Fisher's least significant difference test. $P < 0.05$ was considered significant.

3. Results

3.1 GluK2 receptor endocytosis is likely a clathrin-independent process

There are multiple pathways of internalization from the surface of eukaryotic cells that utilize different mechanisms. Based on the requirement for the coat protein clathrin, these pathways can be divided into clathrin-dependent and clathrin-independent pathways (Mayor and Pagano, 2007; Mousavi et al., 2004). Genistein (Kumar et al., 2019; Li et al., 2020; Pooja et al., 2015; Vercauteren et al., 2010) and MβCD (Guo et al., 2015; Li et al., 2020; Vercauteren et al., 2010; Zhang et al., 2018) are inhibitors of the clathrin-independent pathway; Pitstop2 (Guo et al., 2015; Kumar et al., 2019; von Kleist et al., 2011) and CPZ (Li et al., 2020; Pooja et al., 2015; Vercauteren et al., 2010; Zhang et al., 2018) are commonly used as inhibitors of clathrin-dependent endocytosis. To identify the features of GluK2 endocytosis, cultured primary cortical neurons were pretreated with the above endocytosis inhibitors before kainate stimulation. The concentration of each compound has been justified based on similar applications in the above papers. As shown in Fig. 1A, the kainate-induced reduction in surface GluK2 was prevented by genistein (200 μmol/L) or MβCD (3 mmol/L) but not by pitstop2 (25 μmol/L) or CPZ (10 μmol/L). Genistein treatment and MβCD treatment increased the surface GluK2 by 79.1% and 96.6%, respectively. Endocytosis of transferrin (a marker of the clathrin-dependent process) was used as a control to confirm the specificity and selectivity of these endocytosis inhibitors. As shown in Fig. 1B, MβCD, or genistein treatment did not impair transferrin uptake, but pitstop2 and CPZ did. These results indicate that GluK2 endocytosis is less likely to be a clathrin-mediated process.

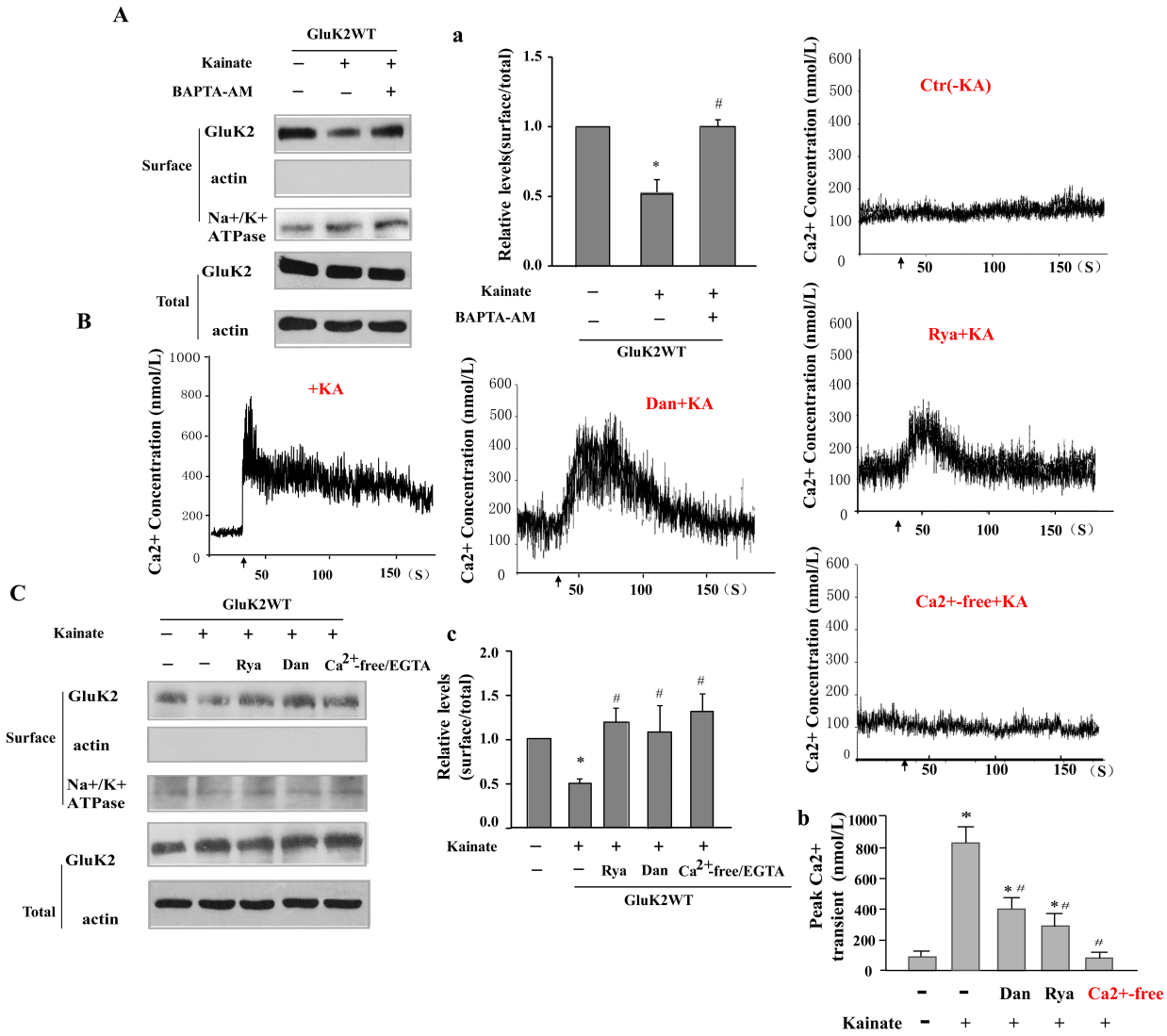

Fig. 2. Ca^{2+} influx and intracellular Ca^{2+} release facilitate GluK2 endocytosis. (A) Membrane localization of GluK2 in transfected HEK293T cells (with or without BAPTA-AM pretreatment). The surface and total GluK2 were examined by immunoblotting with anti-GluK2/3 antibodies. The surface/total ratios of GluK2 are normalized to that of the control (without kainate stimulation) and expressed as the mean ± SD (n = 3). $^{*}P < 0.05$ vs. no kainate. $^{\#}P < 0.05$ vs. no inhibitor in kainate stimulation. (B) Calcium imaging analysis in GluK2-transfected HEK293T cells. Dan (10 μmol/L) or Rya (10 μmol/L) was used to prevent ryanodine receptor opening; Ca^{2+}-free/EGTA buffer was used to block Ca^{2+} influx. All the inhibitors were added 30 min before kainate stimulation (300 μmol/L, 10 min). Data are the mean ± SEM (n = 10); $^{*}P < 0.05$ vs. Control (no kainate). $^{\#}P < 0.05$ vs. no inhibitor in kainate stimulation. (C) Surface biotinylation of GluK2-transfected HEK293T cells (with or without Ca^{2+} inhibition). All the inhibitors were added 30 min before kainate stimulation (300 μmol/L, 10 min). The surface/total ratios are normalized to that of the control (untreated cells expressing wild-type GluK2) and expressed as the mean ± SD (n = 3). $^{*}P < 0.05$ vs. no kainate. $^{\#}P < 0.05$ vs. no inhibitor in kainate stimulation.

3.2 Both Ca^{2+} influx and intracellular Ca^{2+} release facilitate GluK2 endocytosis.

Our previous research has reported that GluK2 tyrosine phosphorylation changes both intracellular Ca^{2+} and GluK2 endocytosis in HEK293T cells (Zhu et al., 2014). Here, we attempted to explore whether there is a correlation between Ca^{2+} and GluK2 endocytosis following kainate stimulation in HEK293T cells. BAPTA-AM, a permeable chelator of free Ca^{2+}, was first used to restrict the intracellular Ca^{2+} concentration. The applied concentration of BAPTA-AM was decided according to similar applications (Brown et al., 2008; Tang et al., 2007; Vomaske et al., 2010). The reduction in the membrane expression of GluK2 was prevented when the cells were pretreated with BAPTA-AM (25 μmol/L) before kainate stimulation compared with non-BAPTA-AM treatment Fig. 2A. The relative surface/total GluK2 in the BAPTA-AM group is 188.7% of the non-BAPTA group. This result suggests the potential roles of intracellular Ca^{2+} in facilitating GluK2 endocytosis. Next, we investigated the mechanism of the peak Ca^{2+} transient after kainate stimulation. The GluK2-transfected HEK293T cells were pretreated with inhibitors of the Rya receptor (dantrolene [Dan] or ryanodine [Rya]). Ca^{2+}-free buffer (LiCl 140 mmol/L, KCl 4 mmol/L, EGTA 10 mmol/L, $MgCl_2$ 1 mmol/L, glucose 10 mmol/L, HEPES 5 mmol/L) was

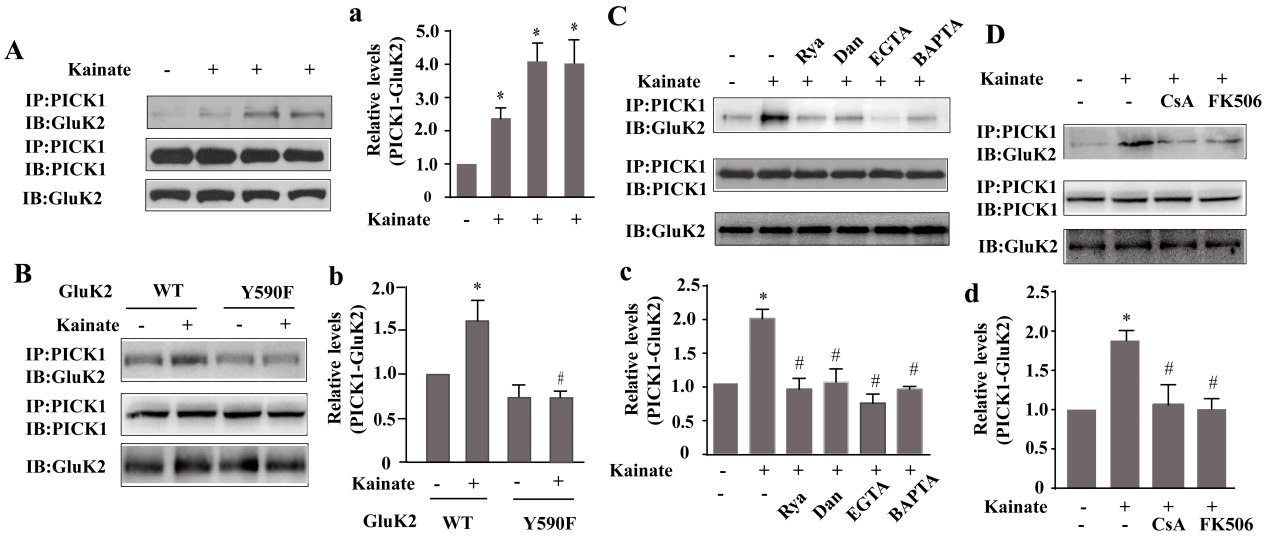

Fig. 3. PICK1 interaction with GluK2 changes and is affected by intracellular Ca^{2+} signaling in kainate stimulation. (A) The interaction of PICK1 with GluK2 increases during kainate stimulation (300 μmol/L for 10 min, 20 min, and 30min) in cultured cortical neurons. (B) The PICK1 interaction with GluK2 in HEK293 cells expressing the wild-type GluK2 (WT) or the tyrosine phosphorylation-deficient mutant Y590F. (C) PICK1-GluK2 binding in cortical neurons is decreased in the presence of calcium inhibitors. $^{*}P < 0.05$ vs. no kainate. $^{\#}P < 0.05$ vs. GluK2 WT without calcium inhibition. The PICK1-GluK2 interactions are normalized to that of the control (without kainate stimulation) and expressed as the mean ± SD (n = 3). $^{*}P < 0.05$ vs. no kainate. $^{\#}P < 0.05$ vs. no inhibitor in kainate stimulation. Neuron cultures for replicates were made from different animals.

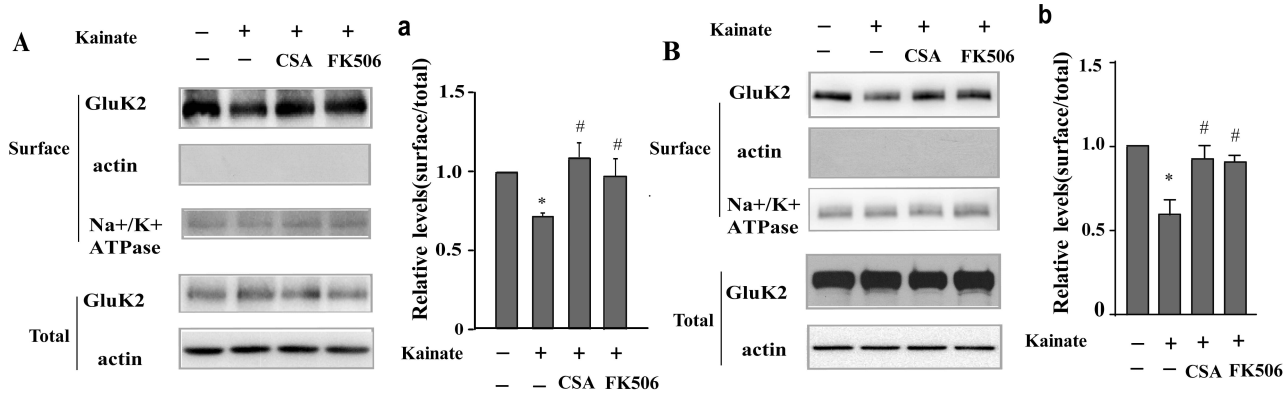

Fig. 4. Calcineurin promotes GluK2 endocytosis. A calcineurin inhibitor (CsA or FK506) prevents the reduction in GluK2 membrane localization during kainate stimulation in GluK2-transfected HEK293T cells (A) and cultured cortical neurons (B). The surface/total ratios are normalized to that of the control and expressed as the mean ± SD (n = 3). $^{*}P < 0.05$ vs. no kainate. $^{\#}P < 0.05$ vs. no inhibitor in kainate stimulation. Neuron cultures for replicates were made from different animals.

used to reduce extracellular Ca^{2+} and impair Ca^{2+} influx. As shown in Fig. 2B, the calcium image analysis showed that the peak Ca^{2+} transient after kainate stimulation was almost abolished in the Ca^{2+}-free group. No significant differences were observed compared with the control group (no kainate stimulation). The peak Ca^{2+} transient was prevented to 404.43 ± 55.72 nmol/L and 280.95 ± 62.08 nmol/L by Dan treatment and Rya treatment, respectively. The peak Ca^{2+} transient in Dan treatment and Rya treatment decreased to 44.8% and 31.2% of that in the kainate stimulation group, respectively. These data demonstrate that both Ca^{2+} influxes from extracellular space and Ca^{2+} release from intracellular stores are necessary for governing the peak Ca^{2+} transient after kainate activation of GluK2. Considering the sources of intracellular Ca^{2+}, the above inhibitors were used to determine the effects of Ca^{2+} on GluK2 endocytosis. As shown in Fig. 2C, relative surface localization of GluK2 in transfected HEK293T cells was 1.1867 ± 0.15567 with Rya treatment (10 μmol/L), 1.3033 ± 0.29092 with Dan treatment (10 μmol/L), and 1.3233 ± 0.19088 with Ca^{2+}-free/EGTA solution treatment. The concentration of Dan or Rya was chosen, referring to several references (Diszházi et al., 2019; Shi et al., 2014; Shinohara et al., 2014; Verkhratsky, 2005). All the treatments significantly inhibited the reduction in surface GluK2 compared to 0.4967 ± 0.05132 in the kainate treatment. The relative surface localization of GluK2 in Rya, Dan, and Ca^{2+}-free/EGTA increased to 238.9%, 262.4%, and 266.4% of that in the kainate stimulation group, respectively.

3.3 PICK1-GluK2 interaction changes under different states of GluK2 endocytosis.

The Ca^{2+} sensor PICK1, a protein with both a PSD-95/Dlg/ZO1 (PDZ) domain and a C-terminal Bin/amphiphysin/Rvs (BAR) domain, has been implicated as a significant component of the machinery that regulates the internalization and trafficking of NMDAR and AMPAR (Fiuza et al., 2017; Hanley and Henley, 2005; Terashima et al., 2008). Here, PICK1-GluK2 binding significantly increased during kainate treatments (300 μmol/L for 10 min, 20 min, and 30 min) Fig. 3A. GluK2 endocytosis was decreased in the group expressing the tyrosine phosphorylation-deficient mutant Y590F (Zhu et al., 2014). Consistent with this finding, the PICK1-GluK2 interaction was reduced in the Y590F group compared with the WT group Fig. 3B. PICK1-GluK2 interaction increased to 160.3% after kainate stimulation. The PICK1-GluK2 interaction after kainate stimulation in the Y590F group decreased to was 46.8% of the WT group.

Peak Ca^{2+} transient is a critical change during kainate stimulation of GluK2, and it is controlled by Y590 phosphorylation (Zhu et al., 2014). Therefore, we attempted to explore whether Ca^{2+} regulates PICK1-GluK2 interaction. Extracellular Ca^{2+} deletion, Rya, Dan, and BAPTA were applied to change the Ca^{2+}sources or intracellular Ca^{2+}concentration. The PICK1-GluK2 interaction was significantly reduced when the cells were pretreated with extracellular Ca^{2+} deletion, Rya, Dan, or BAPTA before kainate stimulation Fig. 3C. The relative levels of the PICK1-GluK2 interaction in the Rya, Dan, EGTA, and BAPTA groups were 0.9200 ± 0.1513, 1.020 ± 0.1873, 0.7200 ± 0.1300, and 0.9167 ± 0.04163, respectively, lower than the level of 1.923 ± 0.1328 in the kainate stimulation group. CaN, a calcium/calmodulin-activated phosphatase has been implicated in several Ca^{2+}-sensitive pathways, including endocytosis (Cousin and Robinson, 2001; Iida et al., 2008). PICK1-GluK2 interaction was also downregulated when CaN was inhibited by CaN inhibitors (CsA and FK-506) Fig. 3D. The PICK1-GluK2 interaction decreased by 43.6% and 46.4% in CsA treatment and FK-506 treatment, respectively. This finding suggests that PICK1 serves as the pivotal effector of the elevated intracellular Ca^{2+} concentration and CaN activation to recruit GluK2.

3.4 CaN activity changes dynamin-dependent GluK2 endocytosis

To study the roles of CaN in GluK2 receptor endocytosis, CaN inhibitors (CsA and FK-506) were administered to inhibit the function of CaN during kainate stimulation. Their concentrations were selected based on application in several references (Koppelstaetter et al., 2018; Takadera and Ohyashiki, 2007; Xu et al., 2012). GluK2 membrane expression was increased when CaN was inhibited Fig. 4A and 4B. CsA treatment and FK-506 treatment caused 47.3% and 31.3% increase of surface GluK2 in HEK293 cells Fig. 4A, respectively. CsA treatment and FK-506 treatment caused 65.5% and 63.1% increase of surface GluK2 in cultured neurons, respectively Fig. 4B. These findings suggest a vital role for CaN in contributing to GluK2 endocytosis.

Clathrin-independent endocytic pathways can either use the scission GTPase dynamin or function independently of this molecule. The surface localization of GluK2 was increased when dynamin activity was inhibited by dynasore Fig. 5A, a cell-permeable inhibitor of dynamin. Dynasore treatment (50 μM and 80 μM) increased the surface localization of GluK2 to 164.8% and 154.2% of that in the kainate stimulation group. Dynamin inhibition likely prevents the process of GluK2 endocytosis. Dynamin1 is expressed in the brain and is enriched in nerve terminals (Smillie and Cousin, 2005). An obvious signal of the GluK2-dynamin1 interaction was observed in the cortical neurons, and the binding of these proteins was decreased in response to inhibition of CaN activity Fig. 5B. CaN inhibition with CsA or FK506 exhibited 65.6% or 72.3% reduction of GluK2-dynamin1 interaction. These findings suggest that GluK2 endocytosis is probably dependent on dynamin activity. Studies have shown that the acceleration of endocytosis depends on the phosphorylation status of dynamin at two specific amino acids, namely, S774 and S778 (Armbruster et al., 2015; Tan et al., 2003). Dynamin phosphorylation at S774 and S778 was also detected when a CaN inhibitor was applied to cultured primary cortical neurons. Dynamin phosphorylation at Ser774 was respectively increased to 208.6% and 188.0% of that in the kainate stimulation group when CsA and FK506 inhibited caN activity, and Ser778 was increased to 213.9% and 195.0% of that Fig. 5C. These results provide evidence that dynamin is the key substrate of CaN in regulating GluK2 endocytosis.

4. Discussion

GluK2 receptor endocytosis has attracted attention because of its roles in synaptic transmission and excitotoxicity, and diverse regulatory processes have been proven to affect this process (Konopacki et al., 2011; Martin et al., 2007; Nasu-Nishimura et al., 2010; Zhu et al., 2014, 2012). Our findings illustrate the mechanisms of GluK2 endocytosis triggered by intracellular Ca^{2+} and Ca^{2+}-activated CaN Fig. 6. Kainate activation induces Ca^{2+} elevation from extracellular and intracellular sources, and subsequently, Ca^{2+}-activated CaN activation enhances PICK1-GluK2 interaction, dynamin-GluK2 binding, and dynamin activity to promote GluK2 endocytosis. These findings provide a detailed understanding of GluK2 receptor endocytosis and identify another potential therapeutic target for treating diseases involving KAR dysfunction, such as stroke.

Here, treatment with specific inhibitors provides important insights into the initial events of GluK2 endocytosis. Both pitstop2 and CPZ inhibit the endocytosis of transferrin, a marker of clathrin-mediated processes, but do not impact GluK2 endocytosis. This finding confirmed that GluK2 endocytosis is different from the clathrin-dependent endocytosis of transferrin. Genistein, a broad-spectrum tyrosine kinase inhibitor, is widely used to inhibit clathrin-independent endocytosis because it interrupts the tyrosine phosphorylation of caveolin by Src kinase (Aoki et al., 1999; Grande-García et al., 2007). GluK2 is also phosphorylated by Src kinase (Zhu et al., 2014), and therefore, the inhibition of GluK2 tyrosine phosphorylation at Y590 cannot be excluded when genistein is applied. Furthermore, the inhibition of GluK2 tyrosine phosphorylation at Y590 also causes a reduction in GluK2 endocytosis (Zhu et al., 2014). MβCD removes cholesterol from cell membranes, thereby disrupting the integrity of caveolae (Zhang et al., 2018). MβCD is another inhibitor of clathrin-independent en-

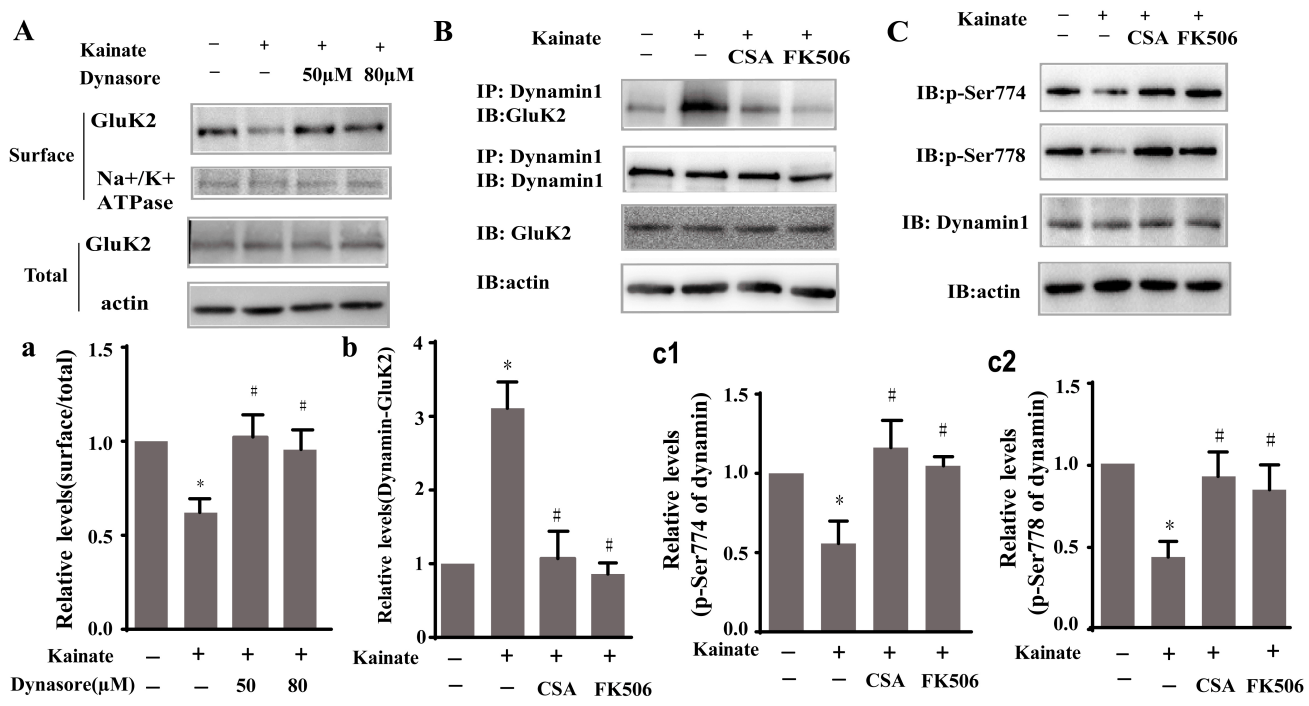

Fig. 5. Dynamin serves as the substrate of CaN and participates in the regulation of GluK2 endocytosis in cultured primary cortical neurons. (A) GluK2 surface localization increases when dynamin activity is blocked by dynasore. The surface/total ratios are normalized to that of the control (without kainate stimulation) and expressed as the mean ± SD (n = 3). $^{*}P < 0.05$ vs. no kainate. $^{\#}P < 0.05$ vs. no dynasore in kainate stimulation. (B) Dynamin binding with GluK2 increases and is decreased by CaN during GluK2 endocytosis. The dynamin-GluK2 interactions are normalized to that of the control (without kainate stimulation) and expressed as the mean ± SD (n = 3). $^{*}P < 0.05$ vs. no kainate. $^{\#}P < 0.05$ vs. no inhibitor in kainate stimulation. Neuron cultures for replicates were made from different animals. (C) Dynamin1 is dephosphorylated at Ser774 and Ser778 by calcineurin. The phosphorylation levels are normalized to that of the control (without kainate stimulation) and expressed as the mean ± SD (n = 5). $^{*}P < 0.05$ vs. no kainate. $^{\#}P < 0.05$ vs. no inhibitor in kainate stimulation. Neuron cultures for replicates were made from different animals.

docytosis. MβCD treatment is necessary to confirm the clathrin-independent process of GluK2 endocytosis. Together with these results from various inhibitors of clathrin-dependent and clathrin-independent endocytosis, our results suggest that GluK2 receptor endocytosis is more likely a clathrin-independent process.

The opening of the channels on the cell surface enables a transient peak of Ca^{2+} influx (Verkhratsky, 2005). Ca^{2+} influx via GluK2 is prevented when the GluK2 function is blocked in the control group without kainate stimulation or other mutant GluK2 groups. Ca^{2+} influx is also blocked when a Ca^{2+} free/EGTA solution replaces the DMEM medium. Dan and Rya do not block surface Ca^{2+} channels but instead reduce intracellular Ca^{2+} release by blocking ryanodine receptors (Adasme et al., 2015; Shi et al., 2014). However, Ca^{2+} entry and intracellular Ca^{2+} release are difficult to separate, since a communication exists between internal compartments and the external Ca^{2+}. Ca^{2+} influx may serve as a trigger to open intracellular Ca^{2+} stores for Ca^{2+}-induced Ca^{2+} release (CICR) during kainate activation, both of which have a contribution to GluK2 endocytosis. There is a limitation to our findings in that the roles of Ca^{2+} in GluK2 endocytosis are illustrated here only in HEK293T cells; however, it is possible that similar results can also be observed in neurons because CaN activation exerts similar effects on GluK2 endocytosis in these two different cell systems Fig. 4A and 4B.

Endophilin and PICK1, BAR domain protein family members, have previously been implicated in clathrin-dependent endocytosis (Fiuza et al., 2017; Vehlow et al., 2013). Especially for ionic glutamate receptor endocytosis, PICK1 has been shown to play a role in the clathrin-mediated endocytosis of GluA2-containing AMPARs (Fiuza et al., 2017). Recently, a role for BAR domain proteins, primarily endophilin, has also emerged in multiple clathrin-independent endocytosis (CIE) pathways (Boucrot et al., 2015; Renard et al., 2015). Our findings reveal a potential role of PICK1 in clathrin-independent GluK2 receptor trafficking.

Dynasore inhibition of dynamin activity increases the surface localization of GluK2, which implies vital roles for dynamin in GluK2 endocytosis. CaN is an obvious candidate for the dynamin phosphatase (Smillie and Cousin, 2005). Ser774 and Ser778 are the phosphorylation sites by which CaN phosphatase regulates dynamin activity. However, dynamin phosphorylation is regulated by a network of phosphatases and protein kinases (Smillie and Cousin, 2005). Ca^{2+}-activated kinases have the potential to form a network with CaN to regulate the dynamin phosphorylation status and GluK2 endocytosis. Therefore, the specific kinases involved in regulating dynamin phosphorylation for GluK2 endocytosis remains to be identified.

The internalized GluK2 can be sorted to recycling or degradation pathways depending on the endocytotic stimulus (Martin and Henley, 2004). It has been speculated that perhaps the internalized GluK2 receptors are recycled for sustained signal trans-

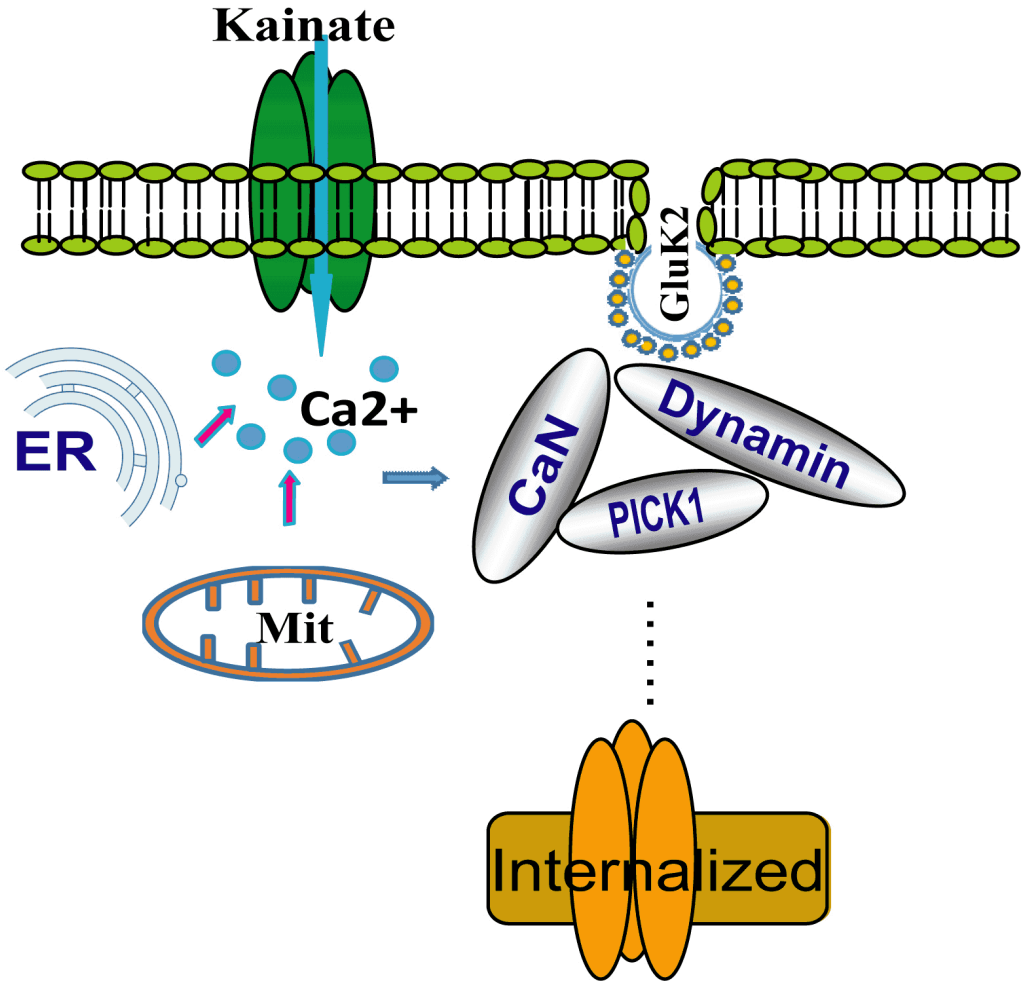

Fig. 6. The Ca^{2+}-elicited pathway mediates a possible mechanism for the regulation of GluK2 endocytosis. GluK2-mediated Ca^{2+} elevation from the influx and intracellular release is involved in GluK2 endocytosis. Ca^{2+} transient and activated CaN activation promotes PICK1 interaction with GluK2. CaN dephosphorylates dynamin and changes dynamin-GluK2 interaction to regulate GluK2 endocytosis.

duction under this stimulus. When exploring GluK2 endocytosis, we just detected the changes in surface GluK2. It is not possible to distinguish endocytosis from recycling in our work, and thus, the trafficking of GluK2 in this process requires additional exploration.

In conclusion, our results demonstrate that the initial events in GluK2 endocytosis. GluK2 is recruited by PICK1, which is elicited by Ca^{2+}/ CaN. CaN activation dephosphorylates the critical GTPase dynamin, promotes GluK2-dynamin binding when facilitating GluK2 endocytosis in excitotoxicity. Our results also provide a theoretical basis for understanding Ca^{2+}/calcineurin signaling in GluK2 receptor endocytosis and will assist in designing drug targets for stroke treatment.

Abbreviations

AMPAR: α-amino-3-hydroxy-5-methyl-4-isoxazolepropionic acid receptor; Ca^{2+}: calcium; CaN: calcineurin; CICR: Ca^{2+}-induced Ca^{2+} release; CIE: clathrin-independent endocytosis; CPZ: chlorpromazine hydrochloride, CsA: cyclosporine A; Dan: dantrolene; KAR: kainate receptor; MβCD: methyl-β-cyclodextrin; NMDAR: N-methyl-d-aspartate receptor; PEI: polyethyleneimine; PICK1: protein-interacting with C kinase 1; Rya: ryanodine; SDS-PAGE: sodium dodecyl sulfate-polyacrylamide gel electrophoresis.

Author contributions

Q-J.Z. designed the research; J.-J.D. L.Y., W. Z., and H.X. performed the research; J.-J.D. L.Y., H.X., and Q.-J.Z. analyzed and interpreted the data; Q.-J. Z wrote the paper.

Ethics approval and consent to participate

This article does not contain any studies with human participants performed by any of the authors. The Animal Research Committee approved all the animal experiments of the Institute of Laboratory Animals, Xuzhou Medical University.

Acknowledgments

This work was supported by the National Natural Science Foundation of China Grant 81501165, the Natural Science Foundation of Jiangsu Province BK20150209, and the Jiangsu Qinglan Project 81473185 and Science and Technology Project of Xuzhou KC19015.

Conflict of Interest

The authors declare no conflicts of interest.

Submitted: April 09, 2020
Revised: September 01, 2020
Accepted: September 14, 2020
Published: September 30, 2020

References

Adasme, T., Paula-Lima, A. and Hidalgo, C. (2015) Inhibitory ryanodine prevents ryanodine receptor-mediated Ca^{2+} release without affecting endoplasmic reticulum Ca^{2+} content in primary hippocampal neurons. *Biochemical and Biophysical Research Communications* **458**, 57-62.

Aoki, T., Nomura, R. and Fujimoto, T. (1999) Tyrosine Phosphorylation of Caveolin-1 in the Endothelium. *Experimental Cell Research* **253**, 629-636.

Armbruster, M., Messa, M., Ferguson, S. M., De Camilli, P. and Ryan, T. A. (2015) Dynamin phosphorylation controls optimization of endocytosis for brief action potential bursts. *Elife* **2**, e00845.

Balaji, J., Armbruster, M. and Ryan, T. A. (2008) Calcium control of endocytic capacity at a CNS synapse. *Journal of Neuroscience* **28**, 6742-6749.

Berliocchi, L., Bano, D. and Nicotera, P. (2006) Ca^{2+} signals and death programmes in neurons. *Philosophical Transactions of the Royal Society of London. Series B, Biological Sciences* **360**, 2255-2258.

Boucrot, E., Ferreira, A. P. A., Almeida-Souza, L., Debard, S., Vallis, Y., Howard, G., Bertot, L., Sauvonnet, N. and McMahon, H. T. (2015) Endophilin marks and controls a clathrin-independent endocytic pathway. *Nature* **517**, 460-465.

Brown, M. V., Burnett, P. E., Denning, M. F. and Reynolds, A. B. (2008) PDGF receptor activation induces p120-catenin phosphorylation at serine 879 via a PKCalpha-dependent pathway. *Experimental Cell Research* **315**, 39-49.

Choi, D. W. (1995) Calcium: still Still center-stage in hypoxic-ischemic neuronal death. *Trends in Neurosciences* **18**, 58-60.

Contractor, A., Swanson, G. and Heinemann, S. F. (2001) Kainate receptors are involved in short- and long-term plasticity at mossy fiber synapses in the hippocampus. *Neuron* **29**, 209-216.

Cousin, M. A. and Robinson, P. J. (2001) The dephosphins: dephosphorylation Dephosphorylation by calcineurin triggers synaptic vesicle endocytosis. *Trends in Neurosciences* **24**, 659-665.

Diszházi, G., Magyar, Z., Mótyán, J. A., Csernoch, L., Jóna, I., Nánási, P. P. and Almássy, J. (2019) Dantrolene requires Mg^{2+} and ATP to inhibit the ryanodine receptor. *Molecular Pharmacology* **96**, 401-407.

Fiuza, M., Rostosky, C. M., Parkinson, G. T., Bygrave, A. M., Halemani, N., Baptista, M., Milosevic, I. and Hanley, J. G. (2017) PICK1 regulates AMPA receptor endocytosis via direct interactions with AP2 α-appendage and dynamin. *Journal of Cell Biology* **216**, 3323-3338.

Fu, X., Yang, Y., Xu, C., Niu, Y., Chen, T., Zhou, Q. and Liu, J. J. (2011) Retrolinkin cooperates with endophilin A1 to mediate BDNF-TrkB early endocytic trafficking and signaling from early endosomes. *Molecular Biology of the Cell* **22**, 3684-3698.

Grande-García, A., Echarri, A., de Rooij, J., Alderson, N. B., Waterman-Storer, C. M., Valdivielso, J. M. and del Pozo, M. A. (2007) Caveolin-1 regulates cell polarization and directional migration through Src kinase and Rho GTPases. *Journal of Cell Biology* **177**, 683-694.

Grynkiewicz, G., Poenie, M., Tsien and R. Y. (1985) A new generation of Ca^{2+} indicators with greatly improved fluorescence properties. *Journal of Biological Chemistry* **260**, 3440-3450.

Guo, S., Zhang, X., Zheng, M., Zhang, X., Min, C., Wang, Z., Cheon, S. H., Oak, M., Nah, S. and Kim, K. (2015) Selectivity of commonly used inhibitors of clathrin-mediated and caveolae-dependent endocytosis of G protein-coupled receptors. *Biochimica Et Biophysica Acta (BBA) - Biomembranes* **1848**, 2101-2110.

Hanley, J. G. and Henley, J. M. (2005) PICK1 is a calcium-sensor for NMDA-induced AMPA receptor trafficking. *The EMBO Journal* **24**, 3266-3278.

Huettner, J. E. (2003) Kainate receptors and synaptic transmission. *Progress in Neurobiology* **70**, 387-407.

Iida, T., Egusa, H., Saeki, M., Yatani, H. and Kamisaki, Y. (2008) PICK1 binds to calcineurin B and modulates the NFAT activity in PC12 cells. *Biochemical and Biophysical Research Communications* **375**, 655-659.

Kerchner, G. A., Wilding, T. J., Huettner, J. E. and Zhuo, M. (2002) Kainate receptor subunits underlying presynaptic regulation of transmitter release in the dorsal horn. *The Journal of Neuroscience* **22**, 8010-8017.

Konopacki, F. A., Jaafari, N., Rocca, D. L., Wilkinson, K. A., Chamberlain, S., Rubin, P., Kantamneni, S., Mellor, J. R. and Henley, J. M. (2011) Agonist-induced PKC phosphorylation regulates GluK2 SUMOylation and kainate receptor endocytosis. *Proceedings of the National Academy of Sciences* **108**, 19772-19777.

Koppelstaetter, C., Kern, G., Leierer, G., Mair, S. M., Mayer, G. and Leierer, J. (2018) Effect of cyclosporine, tacrolimus and sirolimus on cellular senescence in renal epithelial cells. *Toxicology in Vitro* **48**, 86-92.

Kumar, G. A., Karmakar, J., Mandal, C. and Chattopadhyay, A. (2019) Leishmania donovani internalizes into host cells via caveolin-mediated endocytosis. *Scientific Reports* **9**, 12636.

Lerma, J. (2003) Roles and rules of kainate receptors in synaptic transmission. *Nature Reviews Neuroscience* **4**, 481-495.

Li, M., Yan, P., Liu, Z., Cai, D., Luo, Y., Wu, X., Wang, Q., Huang, Y. and Wu, Y. (2020) Muscovy duck reovirus enters susceptible cells via a caveolae-mediated endocytosis-like pathway. *Virus Research* **276**, 197806.

Lu, X., Meima, M. E., Nelson, J. K., Sorrentino, V., Loregger, A., Scheij, S., Dekkers, D. H. W., Mulder, M. T., Demmers, J. A. A., M-Dallinga-Thie, G., Zelcer, N. and Danser, A. H. J. (2016) Identification of the (Pro) renin Receptor as a novel regulator of low-density lipoprotein metabolism. *Circulation Research* **118**, 222-229.

Mackenzie, K. D., Lim, Y., Duffield, M. D., Chataway, T., Zhou, X. F. and Keating, D. J. (2017) Huntingtin-associated protein-1 (HAP1) regulates endocytosis and interacts with multiple trafficking-related proteins. *Cell Signal* **35**, 176-187.

Malinow, R. and Malenka, R. C. (2002) AMPA receptor trafficking and synaptic plasticity. *Annual Review of Neuroscience* **25**, 103-126.

Man, H., Ju, W., Ahmadian, G. and Wang, Y. T. (2000) Intracellular trafficking of AMPA receptors in synaptic plasticity. *Cellular and Molecular Life Sciences* **57**, 1526-1534.

Martin, S. and Henley, J. M. (2004) Activity-dependent endocytic sorting of kainate receptors to recycling or degradation pathways. *The EMBO Journal* **23**, 4749-4759.

Martin, S., Nishimune, A., Mellor, J. R. and Henley, J. M. (2007) SUMOylation regulates kainate-receptor-mediated synaptic transmission. *Nature* **447**, 321-325.

Mayor, S. and Pagano, R. E. (2007) Pathways of clathrin-independent endocytosis. *Nature Reviews Molecular Cell Biology* **8**, 603-612.

Mousavi, S. A., Malerød, L., Berg, T. and Kjeken, R. (2004) Clathrin-dependent endocytosis. *Biochemical Journal* **377**, 1-16.

Mulle, C., Sailer, A., Pérez-Otaño, I., Dickinson-Anson, H., Castillo, P. E., Bureau, I., Maron, C., Gage, F. H., Mann, J. R., Bettler, B. and Heinemann, S. F. (1998) Altered synaptic physiology and reduced susceptibility to kainate-induced seizures in GluR6-deficient mice. *Nature* **392**, 601-605.

Nasu-Nishimura, Y., Jaffe, H., Isaac, J. T. R. and Roche, K. W. (2010) Differential regulation of kainate receptor trafficking by phosphorylation of distinct sites on GluR6. *Journal of Biological Chemistry* **285**, 2847-2856.

Ouardouz, M., Coderre, E., Basak, A., Chen, A., Zamponi, G. W., Hameed, S., Rehak, R., Yin, X., Trapp, B. D. and Stys, P. K. (2009) Glutamate receptors on myelinated spinal cord axons: I. GluR6 kainate receptors. *Annals of Neurology* **65**, 151-159.

Pei, D., Guan, Q., Sun, Y., Zhang, Q., Xu, T. and Zhang, G. (2006) Neuroprotective effects of GluR6 antisense oligodeoxynucleotides on transient brain ischemia/reperfusion-induced neuronal death in rat hippocampal CA1 region. *Journal of Neuroscience Research* **82**, 642-649.

Pooja, S., Pushpanathan, M., Gunasekaran, P. and Rajendhran, J. (2015)

Endocytosis-mediated invasion and pathogenicity of streptococcus agalactiae in rat cardiomyocyte (H9C2). *PLoS One* **10**, e0139733.

Renard, H., Simunovic, M., Lemière, J., Boucrot, E., Garcia-Castillo, M. D., Arumugam, S., Chambon, V., Lamaze, C., Wunder, C., Kenworthy, A. K., Schmidt, A. A., McMahon, H. T., Sykes, C., Bassereau, P. and Johannes, L. (2015) Endophilin-A2 functions in membrane scission in clathrin-independent endocytosis. *Nature* **517**, 493-496.

Sachidhanandam, S., Blanchet, C., Jeantet, Y., Cho, Y. H. and Mulle, C. (2009) Kainate receptors act as conditional amplifiers of spike transmission at hippocampal mossy fiber synapses. *Journal of Neuroscience* **29**, 5000-5008.

Shi, L., Xu, H., Wei, J., Ma, X. and Zhang, J. (2014) Caffeine induces cardiomyocyte hypertrophy via p300 and CaMKII pathways. *Chemico-Biological Interactions* **221**, 35-41.

Shinohara, T., Kim, D., Joung, B., Maruyama, M., Vembaiyan, K., Back, T. G., Wayne Chen, S. R., Chen, P. and Lin, S. (2014) Carvedilol analog modulates both basal and stimulated sinoatrial node automaticity. *Heart and Vessels* **29**, 396-403.

Silva, A. P., Malva, J. O., Ambrósio, A. F., Salgado, A. J., Carvalho, A. P. and Carvalho, C. M. (2001) Role of kainate receptor activation and desensitization on the $[Ca^{2+}]i$ changes in cultured rat hippocampal neurons. *Journal of Neuroscience Research* **65**, 378-386.

Smillie, K. J. and Cousin, M. A. (2005) Dynamin I phosphorylation and the control of synaptic vesicle endocytosis. *Biochemical Society Symposia* **72**, 87-97.

Takadera, T. and Ohyashiki, T. (2007) Caspase-dependent apoptosis induced by calcineurin inhibitors was prevented by glycogen synthase kinase-3 inhibitors in cultured rat cortical cells. *Brain Research* **1133**, 20-26.

Tan, T. C., Valova, V. A., Malladi, C. S., Graham, M. E., Berven, L. A., Jupp, O. J., Hansra, G., McClure, S. J., Sarcevic, B., Boadle, R. A., Larsen, M. R., Cousin, M. A. and Robinson, P. J. (2003) Cdk5 is essential for synaptic vesicle endocytosis. *Nature Cell Biology* **5**, 701-710.

Tang, Q., Jin, M., Xiang, J., Dong, M., Sun, H., Lau, C. and Li, G. (2007) The membrane permeable calcium chelator BAPTA-AM directly blocks human ether a-go-go-related gene potassium channels stably expressed in HEK 293 cells. *Biochemical Pharmacology* **74**, 1596-1607.

Terashima, A., Pelkey, K. A., Rah, J., Suh, Y. H., Roche, K. W., Collingridge, G., McBain, C. J. and Isaac, J. T. R. (2008) An essential role for PICK1 in NMDA receptor-dependent bidirectional synaptic plasticity. *Neuron* **57**, 872-882.

Tymianski, M., Christopher Wallace, M., Spigelman, I., Uno, M., Carlen, P. L., Tator, C. H. and Charlton, M. P. (1993) Cell-permeant Ca^{2+} chelators reduce early excitotoxic and ischemic neuronal injury *in vitro* and *in vivo*. *Neuron* **11**, 221-235.

Vehlow, A., Soong, D., Vizcay-Barrena, G., Bodo, C., Law, A., Perera, U. and Krause, M. (2013) Endophilin, Lamellipodin, and Mena cooperate to regulate F-actin-dependent EGF-receptor endocytosis. *The EMBO Journal* **32**, 2722-2734.

Vercauteren, D., Vandenbroucke, R. E., Jones, A. T., Rejman, J., Demeester, J., De Smedt, S. C., Sanders, N. N. and Braeckmans, K. (2010) The use of inhibitors to study endocytic pathways of gene carriers: Optimization and pitfalls. *Molecular Therapy* **18**, 561-569.

Verkhratsky, A. (2005) Physiology and pathophysiology of the calcium store in the endoplasmic reticulum of neurons. *Physiological Reviews* **85**, 201-279.

Vignes, M. and Collingridge, G. L. (1997) The synaptic activation of kainate receptors. *Nature* **388**, 179-182.

Vomaske, J., Varnum, S., Melnychuk, R., Smith, P., Pasa-Tolic, L., Shuthanandan, J. I. and Streblow, D. N. (2010) HCMV pUS28 initiates pro-migratory signaling via activation of Pyk2 kinase. *Herpesviridae* **1**, 2.

von Kleist, L., Stahlschmidt, W., Bulut, H., Gromova, K., Puchkov, D., Robertson, M., MacGregor, K., Tomilin, N., Pechstein, A., Chau, N., Chircop, M., Sakoff, J., von Kries, J., Saenger, W., Kräusslich, H., Shupliakov, O., Robinson, P., McCluskey, A. and Haucke, V. (2011) Role of the clathrin terminal domain in regulating coated pit dynamics revealed by small molecule inhibition. *Cell* **146**, 471-484.

Wang, Y., Ju, W., Liu, L., Fam, S., D'Souza, S., Taghibiglou, C., Salter, M. and Wang, Y. T. (2004) α -Amino-3-hydroxy-5-methylisoxazole-4-propionic Acid subtype glutamate receptor (AMPAR) endocytosis is essential for N-Methyl-D-aspartate-induced neuronal apoptosis. *Journal of Biological Chemistry* **279**, 41267-41270.

Wu, X. and Wu, L. (2014) The Yin and Yang of calcium effects on synaptic vesicle endocytosis. *Journal of Neuroscience* **34**, 2652-2659.

Wu, X., McNeil, B. D., Xu, J., Fan, J., Xue, L., Melicoff, E., Adachi, R., Bai, L. and Wu, L. (2009) Ca^{2+} and calmodulin initiate all forms of endocytosis during depolarization at a nerve terminal. *Nature Neuroscience* **12**, 1003-1010.

Wu, X., Zhang, Z., Zhao, W., Wang, D., Luo, F. and Wu, L. (2014) Calcineurin is universally involved in vesicle endocytosis at neuronal and nonneuronal secretory cells. *Cell Reports* **7**, 982-988.

Xu, H., Zhang, Y., Sun, J., Wei, J., Sun, L. and Zhang, J. (2012) Effect of distinct sources of Ca^{2+} on cardiac hypertrophy in cardiomyocytes. *Experimental Biology and Medicine* **237**, 271-278.

Xu, Y., Hou, X. Y., Liu, Y. and Zong, Y. Y. (2009) Different protection of K252a and N-acetyl-L-cysteine against amyloid-beta peptide-induced cortical neuron apoptosis involving inhibition of MLK3-MKK7-JNK3 signal cascades. *Journal of Neuroscience Research* **87**, 918-927.

Yao, L. and Sakaba, T. (2012) Activity-dependent modulation of endocytosis by calmodulin at a large central synapse. *Proceedings of the National Academy of Sciences* **109**, 291-296.

Zhang, F., Guo, H., Zhang, J., Chen, Q. and Fang, Q. (2018) Identification of the caveolae/raft-mediated endocytosis as the primary entry pathway for aquareovirus. *Virology* **513**, 195-207.

Zhu, Q., Kong, F., Xu, H., Wang, Y., Du, C., Sun, C., Liu, Y., Li, T. and Hou, X. (2014) Tyrosine phosphorylation of GluK2 up-regulates kainate receptor-mediated responses and downstream signaling after brain ischemia. *Proceedings of the National Academy of Sciences* **111**, 13990-13995.

Zhu, Q., Xu, Y., Du, C. and Hou, X. (2012) SUMOylation of the kainate receptor subunit GluK2 contributes to the activation of the MLK3-JNK3 pathway following kainate stimulation. *FEBS Letters* **586**, 1259-1264.